Prompt particle emission in correlation with fission fragments

Olivier Litaize[1,a], Olivier Serot[1], Loïc Thulliez[1,2], and Abdelaziz Chebboubi[1]

[1] CEA, DEN, Cadarache, 13108 Saint-Paul-lez-Durance, France
[2] CEA, DRF, IRFU, SPhN, Saclay, 91191 Gif-sur-Yvette, France

Abstract. The de-excitation process of primary fission fragments can be simulated with the FIFRELIN Monte Carlo code leading to an estimation of prompt fission observables such as neutron/gamma multiplicities and spectra in correlation with fission fragments. De-excitation cascades are simulated using the notion of nuclear realization following Becvar terminology generalized to neutron/gamma coupled emission. A nuclear realization is a random set of nuclear levels (energy, spin, parity) in association with partial widths for neutron, gamma or electron emission. Experimental data related to electromagnetic transitions in the discrete level region are taken from RIPL-3 database. When nuclear level structure is completely unknown (in the continuum region), level density and strength function models are used. In between these regions, our partial knowledge of nuclear structure is completed by models up to a fixed maximum level density. In this way the whole available experimental information is accounted for. FIFRELIN is ruled by five free input parameters driving the excitation energy sharing, the rotational energy and the spin distribution of primary fission fragments. These five free parameters are determined to match a target observable such as the average total prompt neutron multiplicity ($\overline{\nu}$). Once this procedure is completed, the whole set of fission observables can be compared with experimental results. Obviously the number of observables obtained within this code is higher than what is available from measurements. This code can therefore provide useful insights into the compatibility between models and a whole set of fission observables. In the present work the influence of shell corrections is reported on level densities and prompt fission neutron spectra (PFNS). The impact of the input data such as primary fission fragment total kinetic energy (TKE) is also addressed. Average prompt neutron multiplicity as a function of TKE is also estimated for each mass split and compared to recent measurements. The presence of structures in the calculations (especially for light nuclei) is clearly related to the nuclear level scheme. Various situations occur and an overestimation (or underestimation) of the calculated number of emitted neutrons can be correlated to the light or heavy fragment of a pair and to a restricted energy range. In addition prompt fission gamma spectra (PFGS) are estimated for selected fragment mass ranges and compared to recent measurements. In this way the presence of specific gamma-ray transitions can be established.

1. Introduction

More and more experiments are performed in the field of nuclear physics to improve our knowledge of fission phenomenon and complete the international nuclear databases used in neutron/gamma transport codes. The well known average prompt neutron multiplicity ($\overline{\nu}$) used to determine the effective multiplication factor in a reactor core can be measured as a function of the primary fission fragment mass $\overline{\nu}(A)$ and total kinetic energy $\overline{\nu}$(TKE). Furthermore recent measurements were performed at IRMM concerning total kinetic energy dependence of the multiplicity for given mass splits $\overline{\nu}$(TKE;A) [1] and prompt fission gamma spectra for different mass ranges [2,3]. At Lohengrin mass spectrometer of the Institut Laue-Langevin (ILL) located at Grenoble (France), recent measurements of kinetic energy dependent isomeric ratio are achieved. More than a single average value or a global spectrum, these data allow us to constrain our models, selecting a parameter value among others or accepting/rejecting an hypothesis.

The FIFRELIN Monte Carlo code [4] has the capability to simulate all the post-scission fission observables starting from a restricted set of parameters (devoted to the excitation energy sharing between the two complementary fragments and to the initial spin distribution) and input data such as pre-neutron fission fragment mass yields and kinetic energy distributions. In this paper we have focused the discussion around the average prompt neutron multiplicity as a function of total kinetic energy for a given mass split ($\overline{\nu}$(TKE;A)) and prompt fission gamma spectra for a selected mass range ($PFGS(A)$). In Sect. 2 we briefly remind the models implemented in FIFRELIN and highlight the influence of shell corrections and input data on selected fission observables. Shell corrections have been changed in the present work impacting level density calculation and neutron observables such as the prompt fission neutron spectrum (PFNS) for instance. Average prompt neutron multiplicity is discussed in Sect. 3 while gamma spectra is discussed in Sect. 4. Finally an outlook of the ongoing work is briefly presented.

2. Model

2.1. Reminder of the model

The model used in the FIFRELIN Monte Carlo code has been detailed many times in previous publications and a brief description is given hereafter.

[a] e-mail: olivier.litaize@cea.fr

The first step of the model consists in sampling the fission fragment characteristics [4]:

- mass A,
- nuclear charge Z,
- kinetic energy KE,
- excitation energy E^*,
- J,
- parity π.

Mass and kinetic energy are generally provided by experimenters but can also be taken from an external code such as the GEF code [5]. Charge is sampled using Wahl Z_p model. Excitation energy sharing between two complementary fragments of a binary fission event is obtained by a mass dependent temperature ratio law $R_T(A)$ ruled by two free parameters R_T^{min} and R_T^{max}. The initial spin is sampled from the well known Bethe model involving a spin cut-off parameter. This distribution requires two additional free parameters σ_L and σ_H that can be mass or energy dependent [6]. The last parameter is the fraction of the moment of inertia of a spheroidal rigid body (related to the rotational energy). Finally negative and positive parities are supposed to be equally likely.

The second step consists in decaying the fully characterized excited fragments. The principle of the de-excitation process involves the Becvar's notion of Nuclear Realization [7] generalized to neutron/gamma emission and is detailed in [8]. A detailed description of the code as well as recent important results can be found in [9]. Nevertheless in the present work a modification has to be mentioned: the shell corrections involved in the level density parameter calculation following Ignatyuk's prescription are those of Mengoni-Nakajima (MN) parameterization instead of Myers-Swiatecki (MS) as in the previous works.

2.2. Influence of shell corrections

Both of the shell correction data sets mentioned in Sect. 2.1 are available from RIPL-3 database [10]. Following a comment from a referee, we should explain here that the whole set of parameters involved in level density calculation (including pairing Δ, asymptotic level density parameter $\tilde{a}$) is consistent with Mengoni-Nakajima shell corrections. We have used Myers-Swiatecki shell corrections in previous works because this was recommended in RIPL-2 database and because it is stated in this database that shell correction estimations is less essential for the systematics of the level density parameters (compared to deformations of highly excited nuclei) and in addition the shell corrections that result from MN parameterization do not differ much from the original MS parameterization. Unfortunately, even if these shell corrections are based on the same mass formula, the parameterization slightly changes and can lead to significant differences in level densities. This can be observed in the case of ^{239}U compound nucleus where the shell corrections are estimated to be roughly 1 MeV and 3 MeV respectively for MS and MN parameterization (Fig. 1).

This set of shell corrections is now used by default in the code and the impact can be seen on prompt fission neutron spectra (PFNS) as shown in Fig. 2 for the spontaneous fission of ^{252}Cf. The spectrum is softer

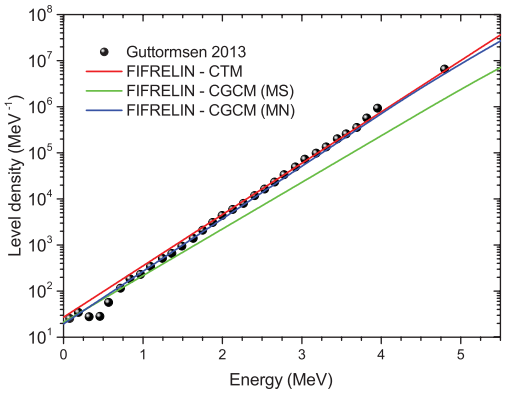

Figure 1. Level density calculated with different models for compound nucleus ^{239}U. Digitized experimental data and CTM parameters used in FIFRELIN come from Guttormsen paper [12]. Calculations with CGCM model and MS shell corrections fail to reproduce data while CGCM with MN shell corrections nicely reproduce them.

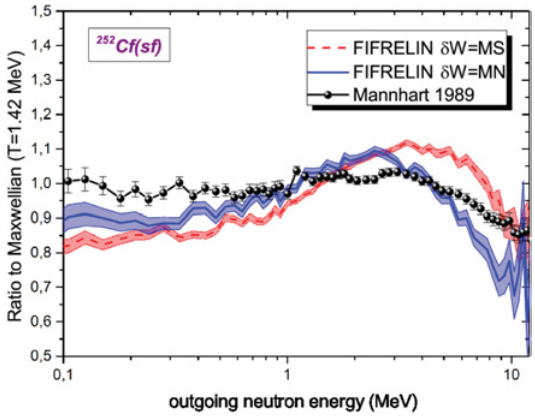

Figure 2. Ratio of PFNS to Maxwellian (T = 1.42 MeV) in the case of ^{252}Cf(sf) reaction. Reference Mannhart evaluation [11] is plotted in black circles, FIFRELIN calculation with Myers-Swiatecki (MS) shell corrections in red dashed line and FIFRELIN calculation with Mengoni-Nakajima (MN) shell corrections in blue line. Shadow area represent the statistical error bar.

($\langle E \rangle = 2.13$ MeV instead of 2.23 MeV previously). The average value is exactly the same as the Mannhart reference [11] but with a stronger component between 1 MeV and 4 MeV while the calculated spectrum is lower at low and high energies.

The increase in level densities favor low energy neutron transitions from one nucleus to its daughter leading to a softer neutron spectrum. The same effect is observed by changing the initial pre-neutron mass, nuclear charge and total kinetic energy distributions. For instance, if the total kinetic energy of primary fission fragments increases, the initial excitation energy is lowered (in average) and high neutron energy transitions are less favored. In addition a lower initial excitation energy is correlated to a lower primary fission fragment spin. Practically the parameters of the temperature ratio law must be changed as well as the spin cut-off parameters that must be lowered in order to recover a consistent average prompt fission neutron multiplicity (target observable). The consequence is a modification of other observable

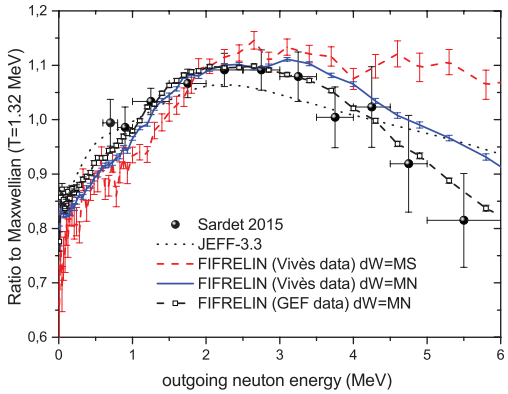

Figure 3. Ratio of FIFRELIN PFNS to Maxwellian (T = 1.32 MeV) for fast fission of ^{238}U at 2.0 MeV. JEFF-3.3/T2 test library file is also represented. The spectrum calculated by FIFRELIN with GEF data (mass yields Y(A), charge yields Y(Z) and total kinetic energy distributions P(TKE;A) is systematically softer than the spectrum calculated with experimental data from [13].

such as the prompt fission neutron spectrum. This effect can be seen in Fig. 3 where input data from GEF code [5] have been used instead of experimental data from Vivès et al. [13] in the case of ^{238}U(n,f) reaction at 2.0 MeV recently measured by Sardet at CEA/DAM/DIF [14]. Calculated average TKE is 170.83 MeV in GEF code compared to 170.01 MeV in experimental data from [13] then the resulting fission spectrum is slightly softer.

3. Prompt fission neutron observables

In this section we focus on average prompt neutron multiplicity as a function of total kinetic energy for given pre-neutron mass splits. This observable was calculated for the whole mass range and all calculated neutron multiplicity curves present structures (plateau corresponding to integer values of $\overline{\nu}$) which can be related to the nuclear level schemes (especially for light fragments with larger spacing between energy levels compared to heavy ones). Figure 4 shows this observable $\overline{\nu}$(TKE;A) for a selection of fragmentation in the pre-neutron mass range A = [103–120; 132–149].

Before going any further, let us consider the specific case of a given fragment (^{104}Nb for instance) as shown in Fig. 5. Starting from the right side of the x-axis to the left side (that means by increasing excitation energy) the number of neutrons emitted goes from 0 to 1, 2, 3 and so on with a series of plateau. This is exactly what we can observe if we plot the number of neutrons emitted as a function of the excitation energy of an excited nucleus, especially if it is spin/parity dependent: $\overline{\nu}(A, Z, E^*, J, \pi)$. In Fig. 5 the width of the first plateau at high TKE corresponding to $\overline{\nu} = 1$ can be related to the energy range in between S_n value of the first daughter (A = 103) and S_n value of nucleus (A = 104), the width of the second plateau ($\overline{\nu} = 2$) at lower TKE is related to the S_n value of the second daughter (A-2) and so on. Obviously this is correct in a first approximation but the situation is a little bit more complicated because it also depends on the spin/parity involved in the neutron transitions. Finally, this is not always clear for each mass split because several nuclear charges, spins, parities can occur. Different situations occur in Fig. 4 with, for instance:

- The calculation of the number of emitted neutrons by the heavy fragment in range A = [139–149] is systematically overestimated at low TKE. This was already observed in the saw-tooth curve [9] but the present work shows that this overestimation is only effective for a restricted low kinetic energy range meaning that models involving high excitation energies could be problematic for these nuclei.
- For heavy fragments near symmetric region A = [132–137] the calculation underestimates the experimental data as already observed in the saw-tooth but here we can see that this arises over the whole energy range systematically. In other words, whatever the excitation energy, the multiplicity is always underestimated questioning the $R_T(A)$ law in this mass range.
- The specific case of mass split 107,145 shows a net inversion of the calculated curves compared to measurements. Surprisingly the agreement is good for the total neutron multiplicity but light fragment emits less neutrons than heavy one, which is exactly the opposite of the measurements. Again, this is the case for the whole TKE range leading to a calculated value of $\overline{\nu}_L/\overline{\nu}_H$ lower than 1 compared to measured value higher than 1.

These data allow to determine if an over/under-estimation of the average neutron multiplicity (saw-tooth curve) is observed and over which total kinetic energy range. Because primary kinetic energy is correlated to primary excitation energy, we can check models on a restricted energy range. For instance when multiplicity is overestimated at low kinetic energy, we can imagine to check level density models in the continuum. Nevertheless this sketch is by far oversimplified, total kinetic energy does not mean single fragment kinetic energy and a mass A contains from 3 to 5 different nuclear charges...

4. Prompt fission gamma observables

This section refers to a preliminary work allowing the determination of fragments at the origin of structures in the prompt fission gamma spectra. Thanks to recent data related to fission gamma-rays of ^{252}Cf(sf) reaction [2], mass dependent gamma spectra have been extracted [3]. We have compared our calculations to these spectra for a restricted primary mass range to check the structures generated by specific intense gamma-ray transitions of the fragments. We focus here on spectrum in correlation with masses A = 128 and A = 129 (with their complementary light partners A = 123 and A = 124) where a structure measured around 500 keV is also observed in the calculation (Fig. 6). A decomposition of the calculated spectrum allows determining that the heavy fragments are not responsible of this structure but their light partners 123 and 124 are good candidates (A = 123 predominantly). Note that these masses are pre-neutron emission masses. Post-neutron emission masses 123, 122 as well as 121 do not emit any gamma near 500 keV (whatever the nuclear charge). If we go further we can show that the post-neutron fragment mass $A^{post} = 120$ associated with a nuclear charge $Z = 48$ emits a prompt gamma at 506 keV.

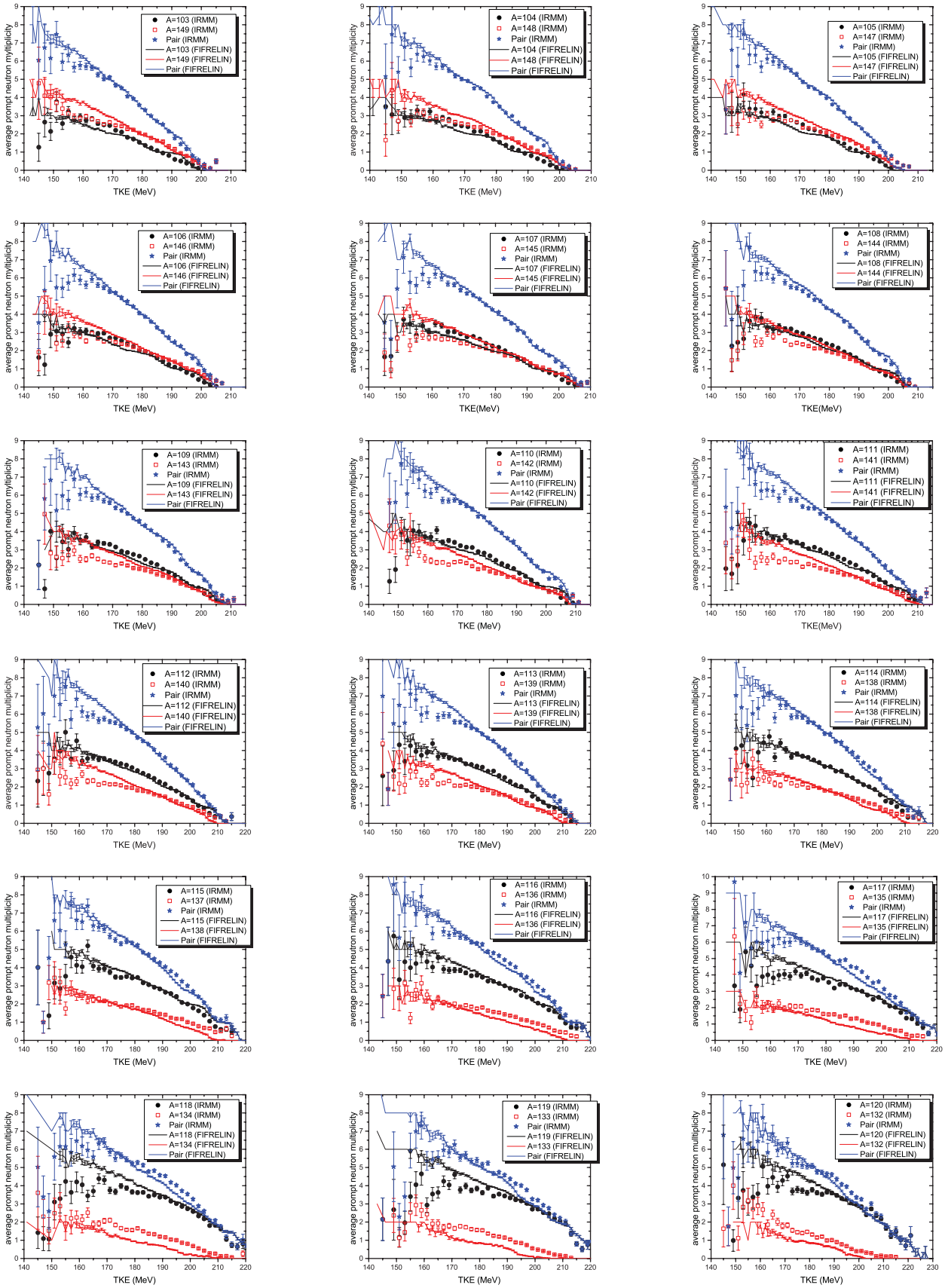

Figure 4. Average prompt neutron multiplicity as a function of total kinetic energy for given mass splits and total average multiplicity for the pair of fragments. Symbols correspond to IRMM experimental data [1] and color lines correspond to FIFRELIN calculations (see text for details).

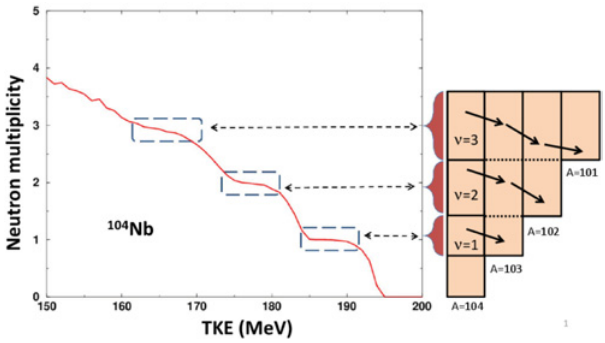

Figure 5. Average neutron multiplicity as a function of TKE for ^{104}Nb. A structure in 'plateau' appears at $\nu = x$ corresponding to energy gap in between $S_n(A - x)$ and $S_n(A - x + 1)$.

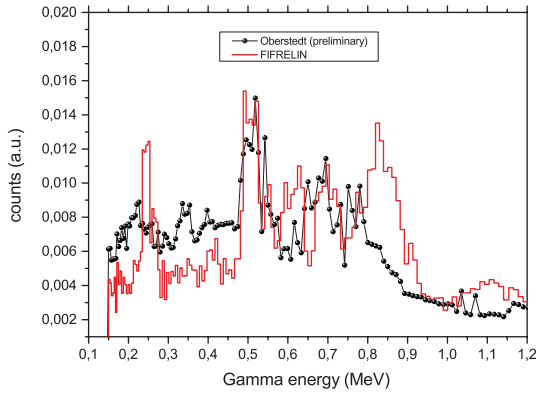

Figure 6. Prompt fission gamma spectrum below 1.2 MeV for ^{252}Cf(sf) reaction. Selected mass range for heavy fragments is A = [128, 129] and A = [123, 124] for complementary light partners.

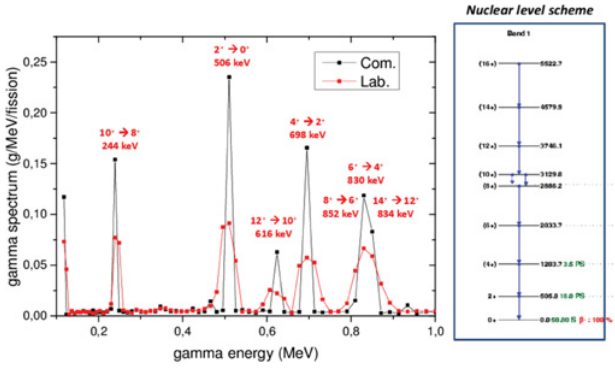

Figure 7. ^{120}Cd gamma spectrum without Doppler correction (in black) and with Doppler correction (in red). The more intense transitions from the ground state band starting from $14^+ \rightarrow 12^+$ accounted for in the code (right side) are obviously visible in the prompt gamma spectrum (left side).

Of course we can verify that the nuclear level scheme of ^{120}Cd coming from RIPL-3 database and used in the code contains a high transition at 506 keV. This is the case of the ground state band (partly reproduced in the right side of Fig. 7) where the intraband transitions from 12^+, 10^+, 8^+, 6^+, 4^+ and 2^+ members are present. The intense transition at 506 keV corresponds to the $(2^+ \rightarrow 0^+)$ transition observed in the calculated spectrum (Fig. 7) as well as in the measured spectrum.

5. Conclusion and outlook

We have shown in this work that the impact of a recent modification in the code (Mengoni-Nakajima shell corrections from RIPL-3 database) allows reproducing level densities of ^{239}U compound nucleus and improving prompt fission neutron spectrum calculations with FIFRELIN. An excellent agreement can be reached by adding a scission neutron component to the fission fragment evaporation process [15].

Average prompt neutron multiplicity in correlation with total kinetic energy and mass of fission fragments have been calculated for the spontaneous fission of ^{252}Cf and compared with recent measurements from IRMM. We can now address if an overestimation or an underestimation is due to the light or the heavy fragment of a fragment pair and which TKE range is affected. Sometimes the calculation fails over the whole TKE range indicating that the temperature ratio law fails for the mass considered. Structures appearing for light fragments are clearly related to the nuclear level scheme (neutron separation energy and energy/spin/parity of levels).

Prompt fission gamma spectra measured for selected mass ranges have been calculated and compared to recent measurements from IRMM. For instance the structure at 500 keV observed in measurements and calculations is predominantly due to pre-neutron mass 123 corresponding to emitting fragment ^{120}Cd (after 3 neutron emission). The nuclear structure used in the code coming from RIPL-3 database is good enough for this nucleus to reproduce the gamma spectrum.

All the calculations performed in this work do not use the tree of events that FIFRELIN can generate on the fly. A specific software has been developed by A. Chebboubi to extract any kind of information from this tree. Work under progress are for instance:

- Kinetic energy dependent Isomeric Ratio measured at LOHENGRIN mass spectrometer located at ILL (Grenoble, France). Regarding the evolution of the isomeric ratio versus the fission fragment kinetic energy, the mechanism for total angular momentum generation is studied [16].
- Yields of correlated fragment pairs measured with the EXILL setup located at ILL on the PF1B neutron guide. For instance the γ-ray intensities in ^{92}Kr and ^{142}Ba in thermal neutron induced fission of ^{235}U are fully consistent between measurements and calculations if the latest (2015) release of RIPL-3 is used at low excitation energy in FIFRELIN code. The evolution of γ-ray intensities in ^{92}Kr versus the complementary partner (Ba) is also compared with calculations but requires a deeper analysis [17, 18].
- Analog fission in neutron transport codes [19]. Shielding calculations are performed with the standard route of TRIPOLI-4 code using nuclear data libraries containing average prompt fission neutron spectra and multiplicities and with the use of fission events generated by FIFRELIN. Fission events consisting in the whole set of caracteristics of a neutron, gamma and conversion electron cascade inside the nuclear level scheme of each fragment allow to consider neutron energy event by event instead of a global spectrum. An impact can be seen on fast reaction rates at surface

positions closest to the fission source and analysis is under investigation.

The authors are greatly indebted to A. Sardet from CEA/DAM/DIF, J.-F. Hambsch and S. Oberstedt from JRC-IRMM for providing useful data and stimulating discussions.

References

[1] A. Göök, F.-J. Hambsch and M. Vidali, Phys. Rev. C **90**, 064611 (2014)
[2] R. Billnert, F.-J. Hambsch, A. Oberstedt and S. Oberstedt, Phys. Rev. C **87**, 024601 (2013)
[3] S. Oberstedt, private communication (2016)
[4] O. Litaize and O. Serot, Phys. Rev. C **82**, 054616 (2010)
[5] K.-H. Schmidt, B. Jurado, C. Amouroux and C. Schmitt, Nucl. Data Sheets **131**, 107 (2016)
[6] L. Thulliez, O. Litaize and O. Serot, Eur. Phys. J. Web Of Conferences **111**, 10003 (2016)
[7] F. Becvar, Nucl. Instrum. Meth. Phys. Res. A **417**, 434 (1998)
[8] D. Regnier, O. Litaize and O. Serot, Comput. Phys. Comm. **201**, 19 (2016)
[9] O. Litaize, O. Serot and L. Berge, Eur. Phys. J. A **51**, 177 (2015)
[10] R. Capote et al., Nuclear Data Sheets **110**, 3107 (2009)
[11] W. Mannhart, in *Properties of Neutron Sources*, Report IAEA-TECDOC-410, 1987, p. 158
[12] M. Guttormsen et al., Phys. Rev. C **88**, 024307 (2013)
[13] F. Vivès, F.-J. Hambsch, H. Bax and S. Oberstedt, Nucl. Phys. A **662**, 63 (2000)
[14] A. Sardet, Thèse de l'Université Paris-Saclay, 2015
[15] O. Serot, O. Litaize, A. Chebboubi, these ND2016 proceedings
[16] A. Chebboubi, G. Kessedjian, O. Litaize, O. Serot, H. Faust, D. Bernard, A. Blanc, U. Köster, O. Méplan, P. Mutti and C. Sage, in Proc. of the 14th Int. Conf. on Nuclear Reaction Mechanism, CERN-Proceedings-2015-001, 33, Varenna, Italy, June 15–19 (2015)
[17] T. Materna, A. Letourneau, C. Amouroux, A. Marchix, O. Litaize, O. Serot, D. Regnier, A. Blanc, M. Jentschel, U. Köster, P. Mutti, T. Soldner, G. Simpson, S. Leoni, G. de France and W. Urban, Eur. Phys. J. Web of Conferences **93**, 02020 (2015)
[18] T. Materna, A. Letourneau, C. Amouroux, A. Marchix, O. Litaize, O. Serot, D. Regnier, A. Blanc, M. Jentschel, U. Köster, P. Mutti, T. Soldner, G. Simpson, S. Leoni, G. de France and W. Urban, these ND2016 proceedings
[19] O. Petit, C. Jouanne, O. Litaize, O. Serot, A. Chebboubi and Y. Pénéliau, in Proc. of Int. Conf. ICRS13 & RPSD 2016, Paris, Oct. 3–6 (2016)